

Six Degree-of-Freedom Localization of Endoscopic Capsule Robots using Recurrent Neural Networks embedded into a Convolutional Neural Network

Mehmet Turan^{a,b}, Abdullah Abdullah^a, Redhwan Jamiruddin^a, Helder Araujo^c, Ender Konukoglu^b, Metin Sitti^a

^a*Physical Intelligence Department, Max Planck Institute, Stuttgart, Germany*

^b*Computer Vision Laboratory, ETH Zurich, Switzerland*

^c*Institute for Systems and Robotics, University of Coimbra, Coimbra, Portugal*

Abstract

Since its development, ingestible wireless endoscopy is considered to be a painless diagnostic method to detect a number of diseases inside GI tract. Medical related engineering companies have made significant improvements in this technology in last decade; however, some major limitations still residue. Localization of the next generation steerable endoscopic capsule robot in six degree-of-freedom (DoF) and active motion control are some of these limitations. The significance of localization capability concerns with the doctors correct diagnosis of the disease area. This paper presents a very robust 6-DoF localization method based on supervised training of an architecture consisting of recurrent networks (RNN) embedded into a convolutional neural network (CNN) to make use of both just-in-moment information obtained by CNN and correlative information across frames obtained by RNN. To our knowledge, our idea of embedding RNNs into a CNN architecture is for the first time proposed in literature. The experimental results show that the proposed RNN-in-CNN architecture performs very well for endoscopic capsule robot localization in cases vignetting, reflection distortions, noise, sudden camera movements and lack of distinguishable features.

Keywords: Endoscopic Capsule Robots, 6 DoF Localization, Deep Learning, Recurrent Neural Networks, Convolutional Neural Networks

1. Introduction

The confinement of present day robot frameworks to make the best use of visual information obstructs their advancement and execution for therapeutic purposes. Conquering this failure would allow robots to execute a countless assortment of crucial roles in human life. However, an essential information required for fulfillment of such tasks is the robot's ability to reliably determine its position in the 3D world. Due to design incompatibility or cost contemplations there arise certain situations where further sensor integration for localization is not possible. Apart from size and cost considerations, the confines also include biocompatibility issues, interference with activation system and limited power availability (Mettin, S., et al., 2015). In such circumstances, vision based methods are a major tool to be used for localization of the robot. The usage of only a monocular endoscope has proved challenging in surgical operations due to the non-rigid deformations. Grasa et al.(2014) researched and provided evidence of the feasibility of monocular endoscopes employed with EKF-SLAM in surgical operations. In-vivo human sequences have been thoroughly studied and validated in (Grasa et al., 2014), e.g. validating the EKF-SLAM in a hernia repair surgical scene. Following the trend, ORB-SLAM was developed for endoscopic tracking and 3D reconstruction (Mur-Artal et al., 2015). However, in all of these methods, the major issue of the requirement for distinguishable landmarks in the scene still remained which is not fulfilled in endoscopic images resulting in a loss of tracking information. Implementation of neural networks for localization of mobile robots is a novel subject and has not been implemented for endoscopic capsule robot localization tasks before. Increasing popularity of CNN in the recent years is associated with the high computational power of modern CPU and GPU technology, and parallel and distributed implementations. Recently, CNNs have been trained with backpropagation (Lecun et al., 1989) which proved to execute fine on large-scale image classification issues (Krizhevsky et al., 2012). At the time of writing we believe our neural network architecture to be the first of its kind to integrate RNN into CNN layers to per-

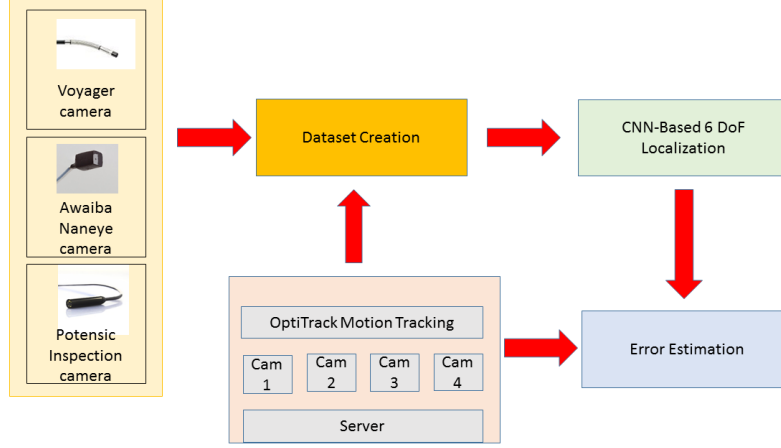


Figure 1: System Diagram

form a robust robot localization. The fact that CNN captures just-in-moment information while RNN is able to remember the correlation between previously occurred and currently occurring patterns makes it useful to combine both concepts for self repeatedly textured areas such as human body inner organs. A dataset consisting of 16000 frames of endoscopic videos was produced using three different endoscopic cameras. The dataset was labeled using OptiTrack, a state-of-the-art optical tracking system for 6 DoF. The setup for the experiment is shown in Figure 2.

2. ALGORITHM ANALYSIS

The algorithm consists of three stages. The first stage addresses the pre-processing of the endoscopic frames and 3D surface reconstruction using shape from shading technique. The second stage implements the scene flow between the 3D maps and the final stage trains the RNN-in-CNN neural network by the estimated scene flow information.

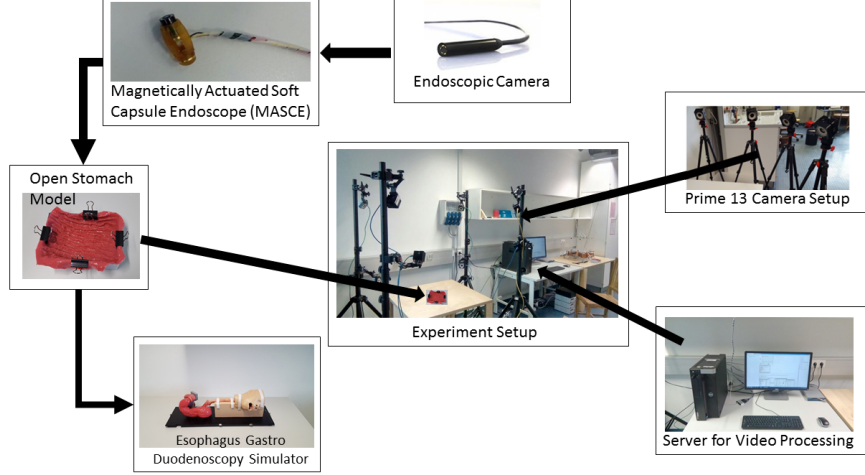


Figure 2: Experimental Setup

2.1. Pre-processing

The algorithm starts with a pre-processing phase in which the consecutive frames follow a number of operations before 3D map reconstruction. Suppression of reflections caused by inner organ fluids, camera calibration, lens-distortion correction and vignetting cancellation are performed at that stage. After these pre-processing stages, shape from shading method of Tsai-Shah (Ruo, Z., et al., 1999) was applied to reconstruct 3D surfaces from 2D endoscopic images. Figure 3 demonstrates a sample depth map created from an endoscopic image using Tsai-Shah method.

2.2. Extraction of the Scene Flow

In this paper the method proposed by Jaimez et al., 2015, is employed to extract the real-time scene flow between the depth images of consecutive frames. In this method the data in the depth images normalizes the flow field that is enforced on the 3D scene surface instead of on the 2D image. The procedure leads to an accurate flow field with geometrically dependable results. Interpolation of the estimated rigid motions is employed to compute velocity of any point

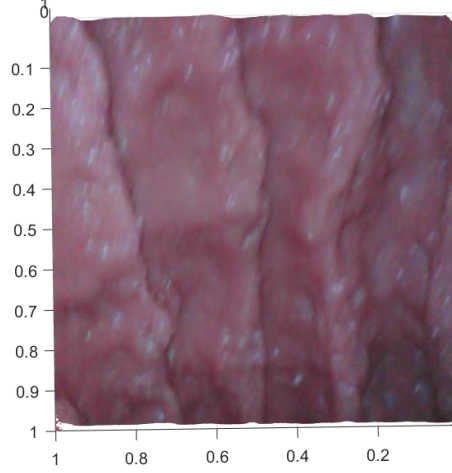


Figure 3: Reconstructed 3D map

and the even parts of the scene and their respective velocities are continuously refined until convergence. Initialization is performed using a k-means-based segmenting and regions are subsequently adapted as the process is optimized to seize any remaining moving parts. The basic objective is to pose scene flow as inference in a conditional random field (CRF). For achieving the task, these steps should be followed:

- The image is partitioned into a set of super-pixels, denoted by S . And the set of objects in the image is denoted by O .
- The super-pixel is associated with a plane variable n describing its 3D geometry and object index is marked with k . This could be written as:

$$i \in S : s_i = (n_i, k_i)^T \quad (1)$$

where normal is $n_i(n_i^T x = 1)$ and object index is k_i

- The second set of variables are defined to capture the rigid motion parameters of all the objects in the scene. This could be written as:

$$Object : i \in O : o_i \in SE(3) \quad (2)$$

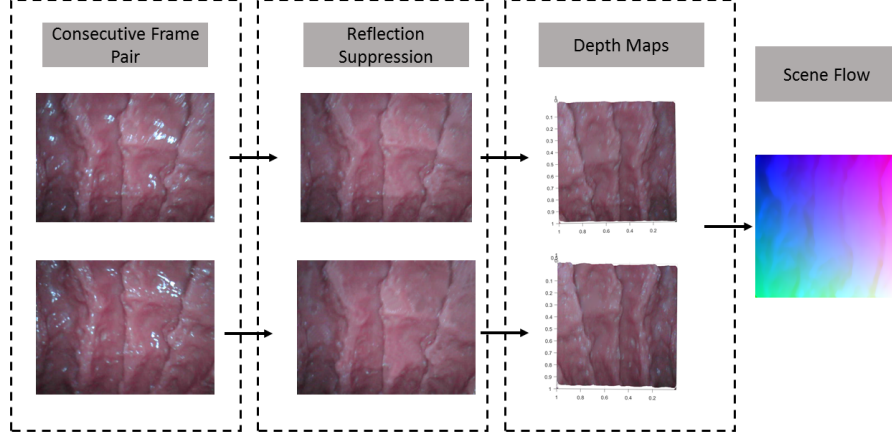


Figure 4: Flow Image Creation

- Finally the objective is formulated in terms of a discrete-continuous CRF energy, comprising of summation of a smoothness and a data term as shown below:

$$E(s, o) = \sum_{i \in S} \varphi_i(s_i, o) + \sum_{i \sim j} \psi_{ij}(s_i, s_j) \quad (3)$$

Structured rigidity is completely captured by binding the scene to be described by only a few objects and max product particle belief propagation is leveraged to approximately minimize the energy.

2.3. A new architecture design: Recurrent neural network embedded into Convolutional neural network

A novel neural network architecture is proposed, which is basically a convolutional neural network with convolutional layers replaced by recurrent neural network layers (RNN) to make use of both just-in-moment information acquired by the CNN and correlations between previous and current frames acquired by RNNs. To our knowledge, the idea of embedding RNN into CNN is for the first

time applied in literature for a robot pose estimation. For estimation of pose values the following loss function was applied in the final layer of the network:

$$loss(I) = ||\hat{x} - x||_2 + \beta ||\hat{q} - \frac{q}{||q||}||_2 \quad (4)$$

To determine the weights of the CNN during backpropagation, stochastic gradient was used. In the above equation, β is a representation of the balance between weights and position. For tracking and achieving optimal results, a value for β is essential to be computed. Since the network is capable of learning the orientation and position simultaneously, these parameters are interrelated and strongly affect the regression of each other.

2.4. Architecture

The neural network architecture implemented in this paper is inspired by PoseNet (Kendall, A., et al., 2015). The proposed architecture however, is significantly different and unique in its implementation. As can be seen in Figure 5, each convolutional module is modified by incorporating RNN layers to the system. The final layer of the proposed architecture is a regressive loss layer instead of a traditional softmax layer to estimate the position and orientation of the robot.

The network was trained with the following parameters:

- GPU: Nvidia K10
- Learning rate: 0.0001
- batch size: 64
- momentum: 0.9
- curve: 90% every 60 epochs
- learning method: stochastic gradient descent

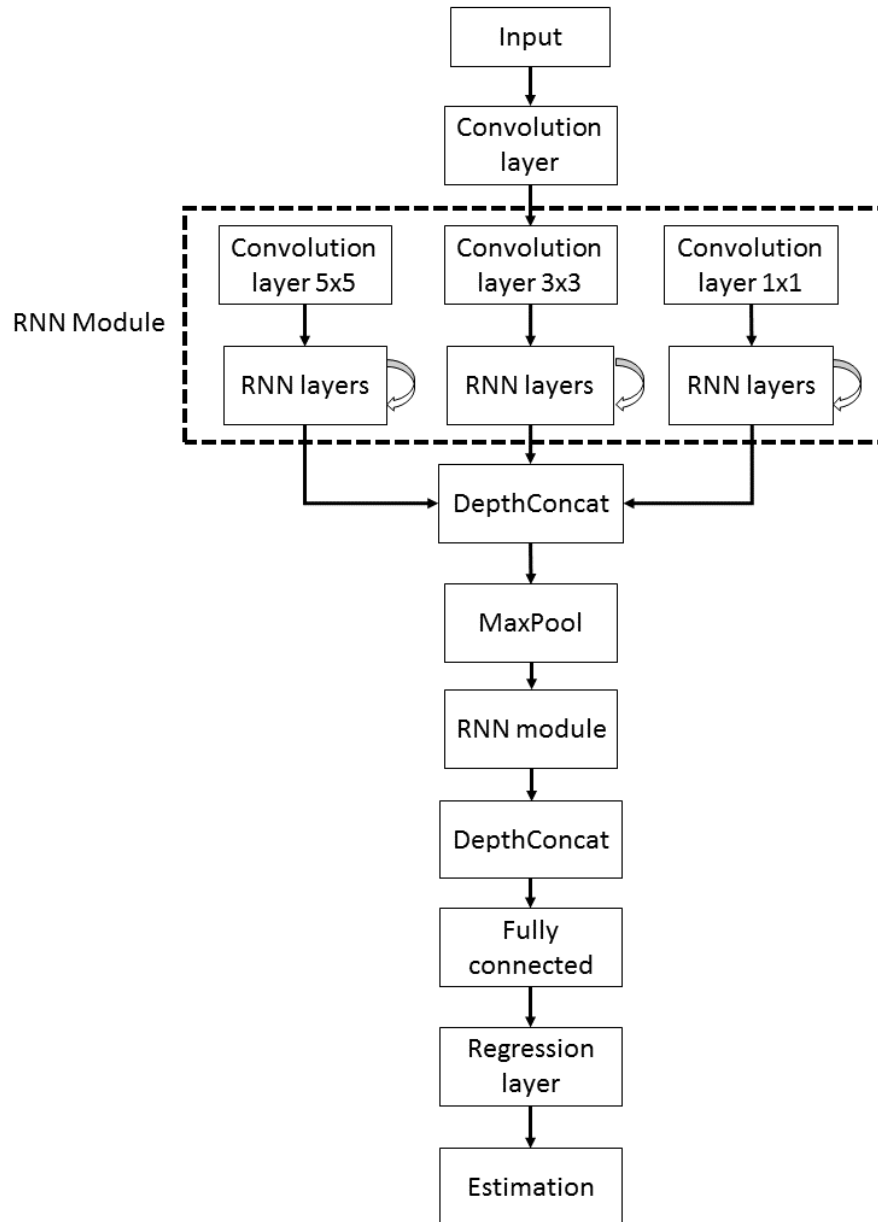


Figure 5: Architecture Block Diagram of the CNN

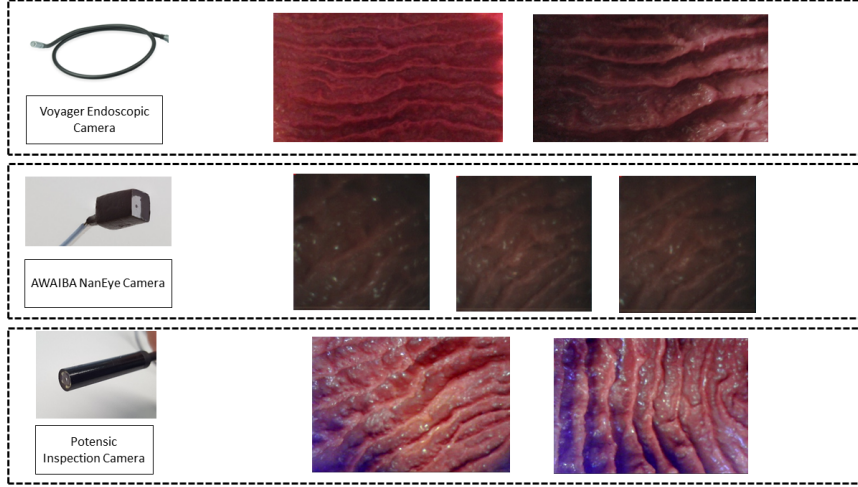


Figure 6: Dataset overview for three different endoscopic cameras.

3. DATASET

The dataset used for testing was recorded in a controlled environment at Max Planck Institute for Intelligent Systems. It was obtained by utilizing esophagus gastro duodenoscopy (EGD) surgical simulator hardware LM-103. EGD is a non-rigid GI Tract model on which paraffin oil had to be applied to imitate the mucosal coat of a real stomach. To prove the fact that the algorithm was not specifically tuned to a single endoscopic camera three different camera models were utilized for video record procedure. The first camera model used was AWAIBA NanEye (see Table 1 and Figure 6). The second camera employed was POTENSIC inspection model (see Table 2 and Figure 6) on the MASCE system. Finally, the last sub-dataset was captured using VOYAGER inspection camera (see Table 3 and Figure 6). The dataset consists of a total of 5 hours long stomach video.

Table 1: AWAIBA NANEYE MONOCULAR CAMERA

Resolution	250 x 250 pixels
Footprint	2.2 x 1.0 x 1.7 mm
Pixel size	3 x 3 μm^2
Pixel depth	10 bit
Frame rate	44 fps

Table 2: POTENSIC MINI MONOCULAR CAMERA

Resolution	1280 x 720 pixels
Footprint	5.2 x 4.0 x 2.7 mm
Pixel size	10 x 10 μm^2
Pixel depth	10 bit
Frame rate	15 fps

Table 3: VOYAGER MINI CAMERA

Resolution	720 x 480 pixels
Footprint	5.2 x 5.0 x 2.7 mm
Pixel size	10 x 10 μm^2
Pixel depth	10 bit
Frame rate	15 fps

4. Trajectory Estimation

Table 4 demonstrates the quantitative results of the trajectory estimation for 7 different trajectories. Trajectory 1 is an uncomplicated path with slow incremental translations and rotations. Trajectory 2 follows a comprehensive scan of the stomach with many local loop closures. Trajectory 3 contains an extensive scan of the stomach with more complicated local loop closures. Trajectory 4 consists of more challenge motions including faster rotational and translational movements. Trajectory 5 consists of very loopy and complex motions with many loop closures. Trajectory 6 is the same of trajectory 5 but included synthetic noise to see the robustness of the system against noise effects. Before capturing trajectory 7, we added more paraffin oil into the simulator tissue to have heavier reflection conditions. Similar to the trajectory 6, trajectory 7 consists of very loopy and complex motions including very fast rotations, translations and drifting. Some qualitative tracking results of our proposed system and corresponding ground truth trajectory sections are demonstrated in figures 7,8,9, and 10. For the quantitative analysis, we used the absolute trajectory (ATE) root-mean-square error metric (RMSE), which measures the root-mean-square of the euclidean distances between all estimated camera poses and the ground truth poses associated by timestamp (Sturm, J., et al., 2012). As seen in table 4, the system performs a very robust and accurate tracking in all of the challenge datasets and is not affected by sudden movements, blur, noise or heavy spectral reflections.

5. Computational performance

To analyze the computational performance of the system we observed the average frame processing time across the trajectory 2 and 4 sequences. The test platform was a desktop PC with an Intel Xeon E5-1660v3- CPU at 3.00, 8 cores, 32GB of RAM and an NVIDIA Quadro P4000 GPU with 8GB of memory. The execution time of the system is depended on the number of surfels in the map,

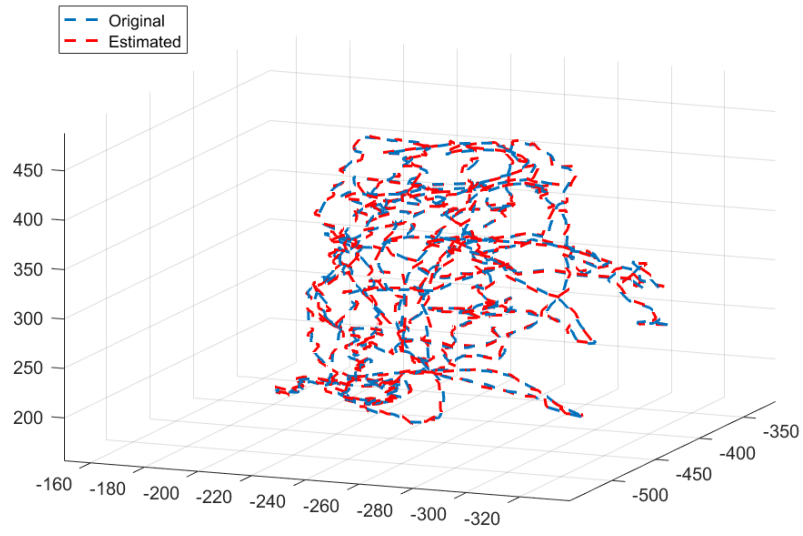


Figure 7: Tracked robot trajectory vs Ground truth 1

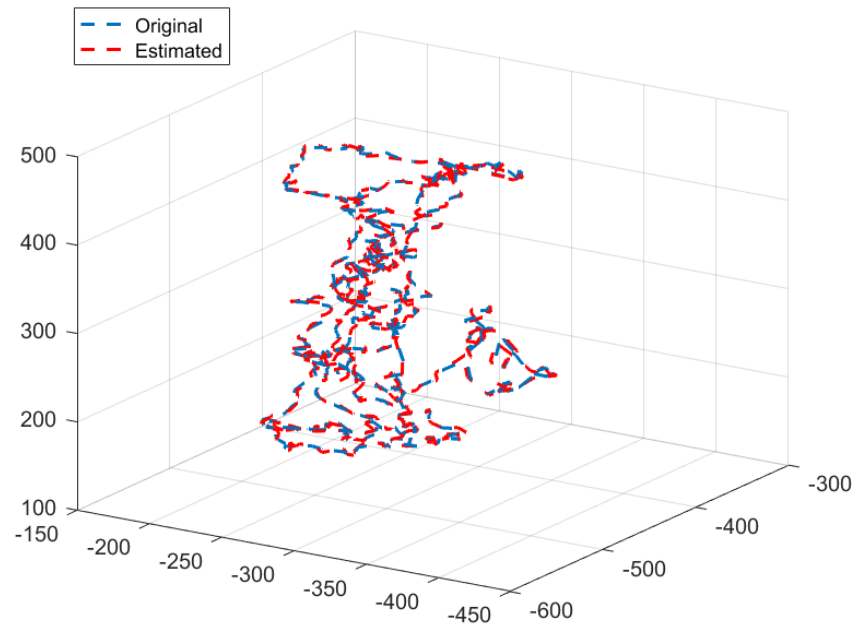


Figure 8: Tracked robot trajectory vs Ground truth 2

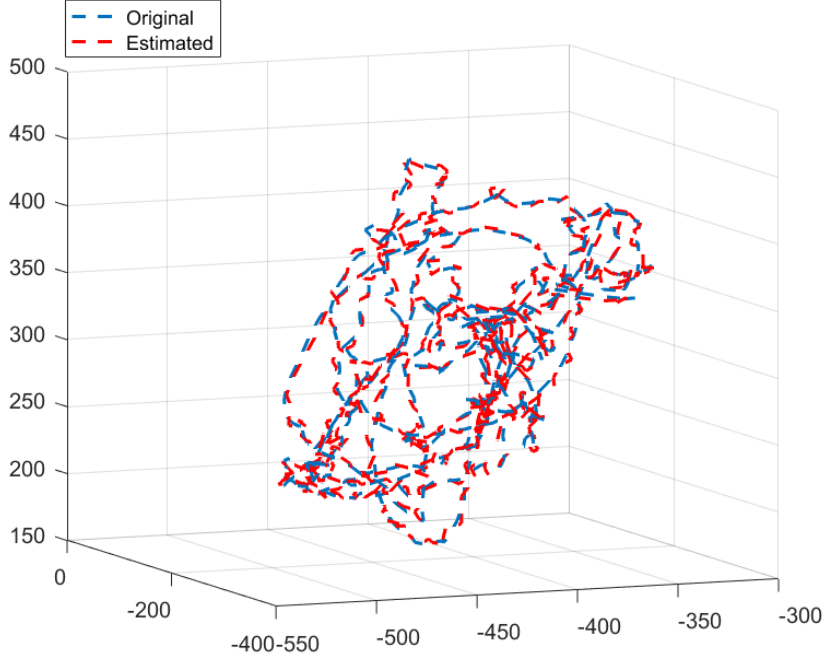


Figure 9: Tracked robot trajectory vs Ground truth 3

Table 4: Trajectory lengths and RMSE results in m

Trajectory ID	POTENSIC	VOYAGER	AWAIBA	LENGTH
1	0.005	0.012	0.0160	0.414
2	0.013	0.015	0.018	0.513
3	0.014	0.016	0.022	0.432
4	0.022	0.025	0.032	0.478
5	0.025	0.028	0.035	0.462
6	0.033	0.036	0.038	0.481
7	0.035	0.040	0.042	0.468

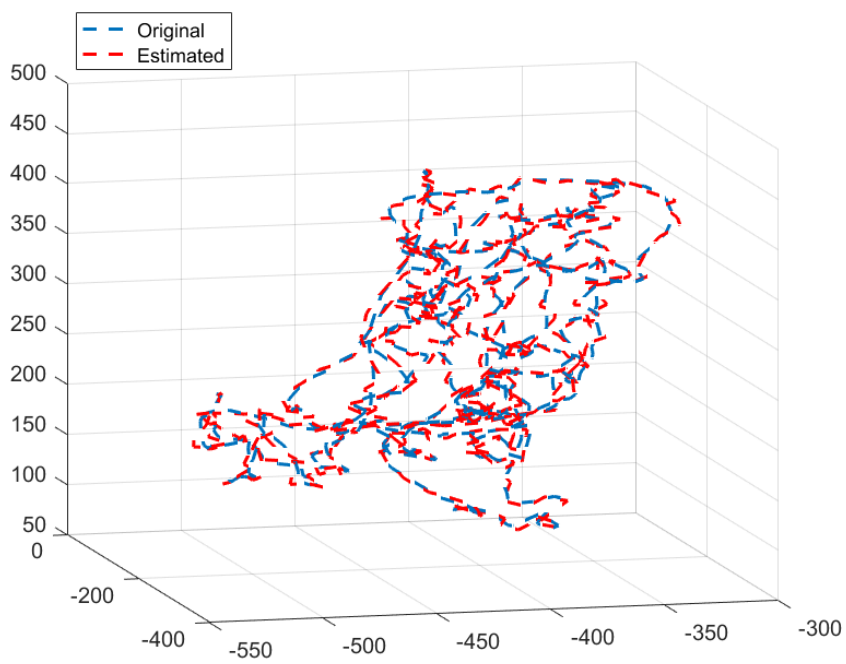


Figure 10: Tracked robot trajectory vs Ground truth 4

with an overall average of 30ms per frame scaling to a peak average of 45ms implying a worst case processing frequency of 22Hz.

6. CONCLUSION

Endoscopic capsule robots are one of the most exiting novel technological developments in the area of medical devices in the last decade. In that paper, we have presented to our knowledge for the first time in literature a deep learning based 6 DoF localization approach for endoscopic capsule robots. The proposed architecture is unique in its kind by embedding RNN layers into the CNN architecture. The proposed system was able to stay close to the ground truth endoscopic capsule robot trajectory even for very challenge datasets confronted with sharp rotations and fast translations, heavy specular reflections and noise. Our system proved qualitatively and quantitatively its effectiveness in occasionally looping capsule robot motions and comprehensive inner organ scanning tasks. In future, we aim to extend our work into the stereo capsule endoscopy applications to achieve even more accurate localization and mapping results.

References

1. Bay, H., et al., 2008. Speeded Up Robust Features: SURF. Computer Vision and Image Understanding, 110, pp. 346-359.
2. Cummins, M., Newman, P., 2008. FAB-MAP: Probabilistic localization and mapping in the space of appearance. The International Journal of Robotics Research, 27, 647-665.
3. Elhabian, Shireen Y. 2008. Hands on shape from shading, Technical report, SCI Home. spring.
4. Engel, J., et al., 2014. LSD-SLAM: Large-scale direct monocular slam. ECCV, pp. 834-849.

5. Forster, C., et al., 2014. Svo: Fast semi-direct monocular visual odometry. Robotics and Automation (ICRA) IEEE International Conference, pp. 15-22.
6. Grasa, O.G., et al., 2014. Visual SLAM for handheld monocular endoscope. IEEE Trans Med Imaging, 33, pp. 135146.
7. Heikkila, J.Silven, O., 1997. A four-step camera calibration procedure with implicit image correction. Proceedings of IEEE Computer Society Conference on Computer Vision and Pattern Recognition.
8. Humphreys, G.W., Bruce, V., 1989. Visual Cognition. Psychology Press, ISBN 0-86377-124-6.
9. Jaimez, M., Souiai, M., Gonzalez-Jimenez, J., Cremers, D., 2015. A primal-dual framework for real-time dense RGB-D scene flow. 2015 IEEE International Conference on Robotics and Automation (ICRA).
10. Jia, Y., et al. Caffe: Convolutional architecture for fast feature embedding. Proceedings of the 22nd ACM international conference on Multimedia.
11. Kaess, M., et al., 2012. iSAM2: Incremental smoothing and mapping using the bayes tree. Int. J. Robotics Res., 31, pp. 217236.
12. Kendall, A., et al., 2015. PoseNet: A Convolutional Network for Real-Time 6-DOF Camera Relocalization. ICCV, pp. 2938-2946.
13. Kingma, D., Jimmy, B., 2014. Adam: A method for stochastic optimization. arXiv, 1412.6980.
14. Klein, G., and Murray, D., 2007. Parallel tracking and mapping for smaller workspaces. ISMAR 2007, IEEE and ACM International Symposium, pp. 225234.
15. Konda, K., Memisevic, R., 2015. Learning visual odometry with a convolutional network. International Conference on Computer Vision Theory and Applications.
16. Lecun, Y., et al., 1989. Backpropagation applied to handwritten zip code recognition. Neural Comput., 1 pp. 541551.

17. Lecun, Y., et al., 2016. Gradient-based learning applied to document recognition. *Proceedings of the IEEE*, 86, pp. 2278-2324.
18. Lowe, D.G., 2004. Distinctive Image Features from Scale-Invariant Keypoints. *IJCV*, 60, pp. 91-110.
19. Mur-Artal, R., et al., 2015. ORB-SLAM: A versatile and accurate monocular SLAM system. *IEEE Trans. Robot.*, 31, pp. 1147-1163.
20. Newcombe, R. A., et al., 2011. DTAM: Dense tracking and mapping in real-time. *ICCV, IEEE International Conference*, pp. 2320-2327.
21. Mettin, S., et al., 2015. Biomedical Applications of Untethered Mobile Milli/Microrobots. *Proceedings of the IEEE*, 103(2).
22. Pirker, K., et al., 2011. CD SLAM, continuous localization and mapping in a dynamic world. *International Conference on Intelligent Robots and Systems*, pp. 3990-3997.
23. Ruo, Z., Tsai, P., Cryer, J., Shah, M., 1999. Shape-from-shading: a survey. *IEEE Transactions on Pattern Analysis and Machine Intelligence* 21, 690-706.
24. Shi, J., Tomasi, C., 1994. Good Features to Track. *IEEE Conference on Computer Vision and Pattern Recognition. CVPR94*, Seattle.
25. Son, D., et al., 2016. A 5-D Localization Method for a Magnetically Manipulated Untethered Robot Using a 2-D Array of Hall-Effect Sensors. *Mechatronics IEEE/ASME Transactions*, 21, pp. 708-716.
26. Stoyanov, D., et al., 2010. Real-Time Stereo Reconstruction in Robotically Assisted Minimally Invasive Surgery. *Medical Image Computing and Computer Assisted Intervention Springer*, pp. 275-282.
27. Sturm, J., Engelhard, N., Endres, F., Burgard, W., Cremers, D., 2012. A benchmark for the evaluation of rgb-d slam systems, in: *Intelligent Robots and Systems (IROS). IEEE/RSJ International Conference on IEEE*, pp. 573-580.
28. Sunderhauf, N., et al., 2015. On the performance of convnet features for place recognition. *arXiv*, 1501.04158.

29. Szegedy, C., et al., 2014. Going deeper with convolutions. arXiv, 1409.4842.
30. Wu, Z., et al. "A gpu implementation of googlenet."
31. Yim, S., et al., 2014. Biopsy using a Magnetic Capsule Endoscope Carrying, Releasing, and Retrieving Untethered Microgrippers. IEEE Trans Biomed Eng, 61, pp. 513-521.
32. Yuanjie, Z., 2008. Single-image vignetting correction using radial gradient symmetry. IEEE Conference on Computer Vision and Pattern Recognition.
33. Mehmet, T., et al., 2017. A Non-Rigid Map Fusion-Based RGB-Depth SLAM Method for Endoscopic Capsule Robots. arXiv:1705.05444 [cs.CV].
34. Mehmet, T., et al., 2017. A Deep Learning Based 6 Degree-of-Freedom Localization Method for Endoscopic Capsule Robots. arXiv:1705.05435 [cs.CV].